



The characteristics of radon and thoron concentration from soil gas in Shenzhen City of Southern China

Nanping Wang,
Ling Zheng,
Xingming Chu,
Shijun Li,
Shouliang Yan

Abstract. Radon (^{222}Rn) and thoron (^{220}Rn) from soil gas are very significant factors that can affect the indoor radon level in the first floor or in the basement. China is one of the countries with the highest thorium content in the world. Therefore, it is very significant to study $^{222}\text{Rn}/^{220}\text{Rn}$ concentration in the soil in Shenzhen City (SC). A $^{222}\text{Rn}/^{220}\text{Rn}$ survey was performed using a portable radon monitor (model RAD7) at 69 sites, covered a total area of 1800 km² in 2013 to get the original data for radon risk estimation in SC. The average values of ^{222}Rn and ^{220}Rn concentration of soil gas of the total 69 locations are 86 ± 72 kBq·m⁻³ and 118 ± 85 kBq·m⁻³, respectively. $^{222}\text{Rn}/^{220}\text{Rn}$ concentrations are related to geological lithology. ^{222}Rn concentrations vary from 40 to 370 kBq·m⁻³ and from 15 to 118 kBq·m⁻³ in weathered granite products and sediments, respectively, while ^{220}Rn concentrations are from 103 to 435 kBq·m⁻³ and 2.2 to 96 kBq·m⁻³. The higher ^{220}Rn values were mainly observed at the sites covered by the weathered granite products. Comparing with the areas of high ^{222}Rn concentration, the areas of high ^{220}Rn values are larger. The distribution of ^{222}Rn concentration in the vertical direction displays an exponential distribution mode, but there is no rule of ^{220}Rn concentration. The investigation suggests that people should pay attention to ^{220}Rn contribution in the radon mapping of SC, as well as in the indoor radon survey.

Key words: $^{222}\text{Rn}/^{220}\text{Rn}$ • soil gas • radon mapping • China

Introduction

As we know, radon is one kind of natural radioactive inert gas, decayed from radium, and its radiation hazard can lead to the increase in the incidence of human' lung cancer. The annual effective dose due to Rn and its products is about 1.2 mSv, which is more than a half fraction of the natural radiation exposure to humans per year [1]. Compared with ^{222}Rn , the researches on ^{220}Rn were not many.

In 1991, an article reported that indoor ^{220}Rn concentrations in the wooden houses with soil wall were significantly higher than that in other types of buildings [2, 3] in Japan. Since then, scientists in China, Germany and the United States have begun to pay attention to the problems caused by high level of indoor ^{220}Rn and its progenies in Yangjiang City (YC) and Zhuhai City (ZC) in Guangdong Province, and Pingliang in Gansu Province of China [4–8]. In 1996, spatial and temporal variations of soil gas ^{222}Rn and ^{220}Rn at two sites were conducted in New Jersey [9].

In recent years, monitoring ^{222}Rn and ^{220}Rn anomalies to study of fault and volcanic activity has aroused people's interest. In Poland, the detail $^{222}\text{Rn}/^{220}\text{Rn}$ measurements were conducted on the surface, and at the depth of 10, 40, and 80 cm below the ground. They found that the concentration versus depth

N. P. Wang[✉], L. Zheng, X. M. Chu, S. J. Li, S. L. Yan
China University of Geosciences (Beijing),
29 Xueyuan Road, Haidian District, Beijing, 100083,
China,
Tel.: +86 10 8232 1833, Fax: +86 10 6368,
E-mail: npwang@cugb.edu.cn

Received: 29 November 2015
Accepted: 29 March 2016

profiles for ^{222}Rn differed from soils developed on fault zones, uranium deposits or both [10]. Soil radon concentrations in the Amer fault zone have been measured for a 4-year period to check seasonal fluctuations and to understand radon origin and dynamics. Radon fluctuations were repeated every year, with values in summer much higher than in winter [11]. Continuous soil gas $^{222}\text{Rn}/^{220}\text{Rn}$ measurements were carried out along Mat fault in Mizoram, and positive correlations were found between $^{222}\text{Rn}/^{220}\text{Rn}$ data and the earthquakes [12]. Anomalous behaviours in radon concentrations have been observed prior to some earthquakes [13]. The measurements of soil gas $^{222}\text{Rn}/^{220}\text{Rn}$, together with carbon dioxide (CO_2) efflux, were performed in the fault zone near the village of Santa Venerina (SV) in the east flank of Mt. Etna volcano to investigate how fractures in the ground can affect the radon transport [14]. Spain scholars researched on soil gas radon emissions and volcanic activity at El Hierro (Canary Islands) [15]. The measurements of the $^{222}\text{Rn}/^{220}\text{Rn}$ exhalation rate were also of concern [16, 17]. $^{222}\text{Rn}/^{220}\text{Rn}$ levels of soil-gas were carried out in Al-Kufa City in Iraq [18].

In 2011, we conducted a $^{222}\text{Rn}/^{220}\text{Rn}$ survey in soil gas by the RAD7 monitor in the period of ZC's radon potential mapping and mapped the first thoron contour map [19]. We noticed that the highest dose rate reached to 368 nGy/h in SC [20]. So a preliminary investigation of $^{222}\text{Rn}/^{220}\text{Rn}$ concentration of soil gas in Shenzhen City (SC) was carried out using a portable semiconductor radon monitor RAD7 in 2013.

Our purposes are:

1. To get the original data for radon mapping and radon risk estimation in SC.
2. To get the information about the level and characteristics of $^{222}\text{Rn}/^{220}\text{Rn}$ in soil gas in SC.
3. To understand the relationship between ^{222}Rn and ^{220}Rn and lithology.

Instruments and methods

Radon monitor and its calibration

^{222}Rn and ^{220}Rn concentrations in the soil gas were determined by a RAD7, radon monitor in SC, manufactured by DurrIDGE Co., Inc. (Bedford, MA). The structure and detector of RAD7 radon monitor were described detail in the article [19].

RAD7 was calibrated at DurrIDGE's indoor calibration facility, which was a radon chamber used radium (^{226}Ra) source to provide RAD7 with ^{222}Rn source. According to the RAD7 User Manual [21], the reproducibility is generally better than 2% with standard RAD7 calibration in DurrIDGE Co. Inc. Overall calibration accuracy is in the range of 5%. The calibration uncertainty of our RAD7 was 2% (1-sigma), and the mean radon concentration in the radon chamber was 1.28 kBq/m³ and the mean Celsius temperature was 24.9, and not including the uncertainty of the reference source which was evaluated to be within $\pm 5\%$ (1-sigma).

The RAD7 was calibrated in a standard radon chamber in the Division of Radioactivity Exploration

Metrology belonged to the Aerial Remote Sensing Center of Chinese National Nuclear Corporation before we started our field measurement in SC.

The 'sniff' mode of the RAD7 was used in radon measurements in the field. Sampling time was 3 min and the pump was set in 'auto' mode. The relative humidity was lower than 10% during field radon investigation. A simple schematic diagram of soil gas radon measurement with RAD7 monitor was shown as in our article [19].

Radon measurement in the field

^{222}Rn and ^{220}Rn measurements were conducted at the depth of 80 cm below the ground. The ^{222}Rn and ^{220}Rn sampling model and the procedure as same as we did in radon survey in Zhongshan City, Guangdong Province [19].

Radon contour map

In order to display the distribution of ^{222}Rn and ^{220}Rn concentration at the depth of 80 cm below ground, a radon contour map was built using Kringing of special grading method. After calculating the original grid values, the spline smooth, using cubic spline interpolation, computed new grid nodes. The interpolation simulates a drafting technique where a flexible strip (a spline) is used to draw a smooth curve between data points.

Overview of investigation area

The surveyed area covered 1800 km², from 113°46' E to 114°37' E, and from 22°27' N to 22°52' N. There is a subtropical oceanic climate with the average annual temperature of 22.4°C in SC.

There are three types of geomorphology in SC, including mountain, tableland and coastal area. The Quaternary strata are composed of gravel, sand, clay and silt. Magmatic activity was very intense during the Yanshanian period in this area. The outcrop areas of the Yanshanian granitoids and volcanic rocks cover up to about 56% of the entire area. Volcanic rocks are mainly composed of the Mid-Jurassic and the Late Jurassic rocks. The intrusive rocks are composed of the Middle and the Late Jurassic and the Cretaceous biotitic granite and granodiorite [22, 23].

A simplified geological map extracted from a 1/500 000 digital geological map database of China Geological Survey (CGS) is shown in Fig. 1.

Characteristics of $^{222}\text{Rn}/^{220}\text{Rn}$ concentration

Radon, thoron, radium and thorium in the vertical direction

In our radon survey, two typical experimental sites were chosen to do a research on the characteristics of $^{222}\text{Rn}/^{220}\text{Rn}$ concentration of soil gas in the vertical

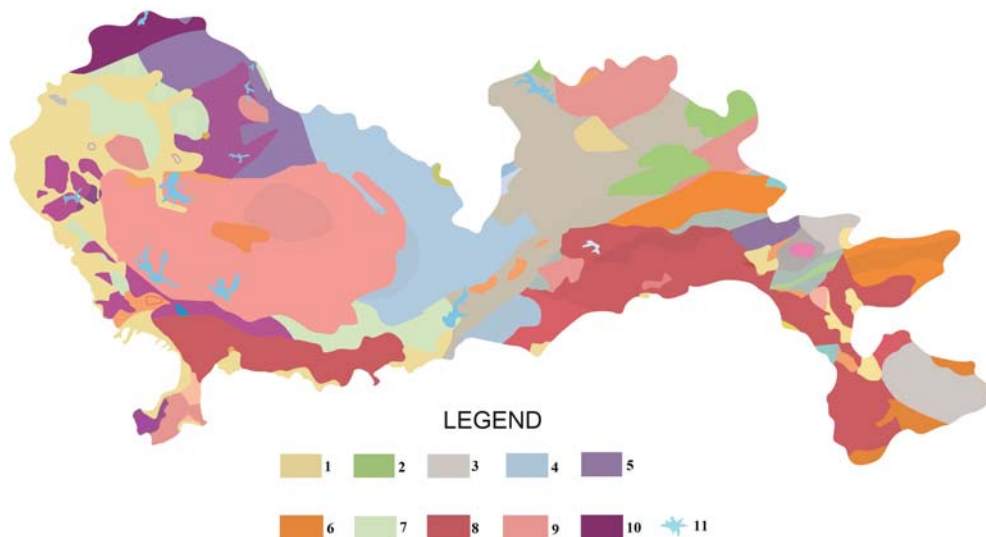


Fig. 1. A simplified geological map of Shenzhen City. 1. Quaternary: gravel, sand, clay, silt and peat. 2. Cretaceous: granitic conglomerate. 3. The Jurassic: tuff, rhyolite, feldspar-quartz sandstone, mudstone, siltstone, conglomerate. 4. The Lower Carboniferous: quartz sandstone, siltstone, slate, metamorphosed siltstone. 5. Triassic: gray conglomerate, sandstone and siltstone, black carbonaceous shale. 6. The Upper Devonian: schist, quartz sandstone. 7. Sinian: fine-grained plagioclase gneiss, quartzite, schist. 8. The Early Cretaceous and the Later Jurassic: fine and fine to coarse grained porphyritic biotite granite. 9. The Middle Cretaceous: fine and medium grained porphyritic monzogranite; the Later Cretaceous fine granite; the Later Jurassic fine and medium grained porphyritic monzogranite. 10. Migmatitic granite. 11. Water reservoir.

direction. One was a site covered with weathered granite, coded as LWS (natural weathered granite outcrops), and the other was located at Wutongshan Mountain coded as WTS, covered with soil. $^{222}\text{Rn}/^{220}\text{Rn}$ concentration was determined by the RAD7 monitor at different depths with vertical intervals of 0.2 m at the same site. Meanwhile, two soil samples were collected at every depth for determining of radium and thorium by HPGe gamma-ray spectrometer in the laboratory. The measuring results are shown in Fig. 2.

Figure 2 shows the following three points:

1. The distribution of ^{226}Ra and ^{232}Th is uniform at the two sites in the vertical direction. The average value of radium specific radioactivity concentration of the total 9 samples is $101 \pm 7.8 \text{ Bq/kg}$, and that thorium specific radioactivity concentration is $127 \pm 17.1 \text{ Bq/kg}$.
2. The distribution of ^{222}Rn concentration in soil gas in the vertical direction is the exponential distribution mode, which can be explained by the diffusion of radon in the soil, but there is

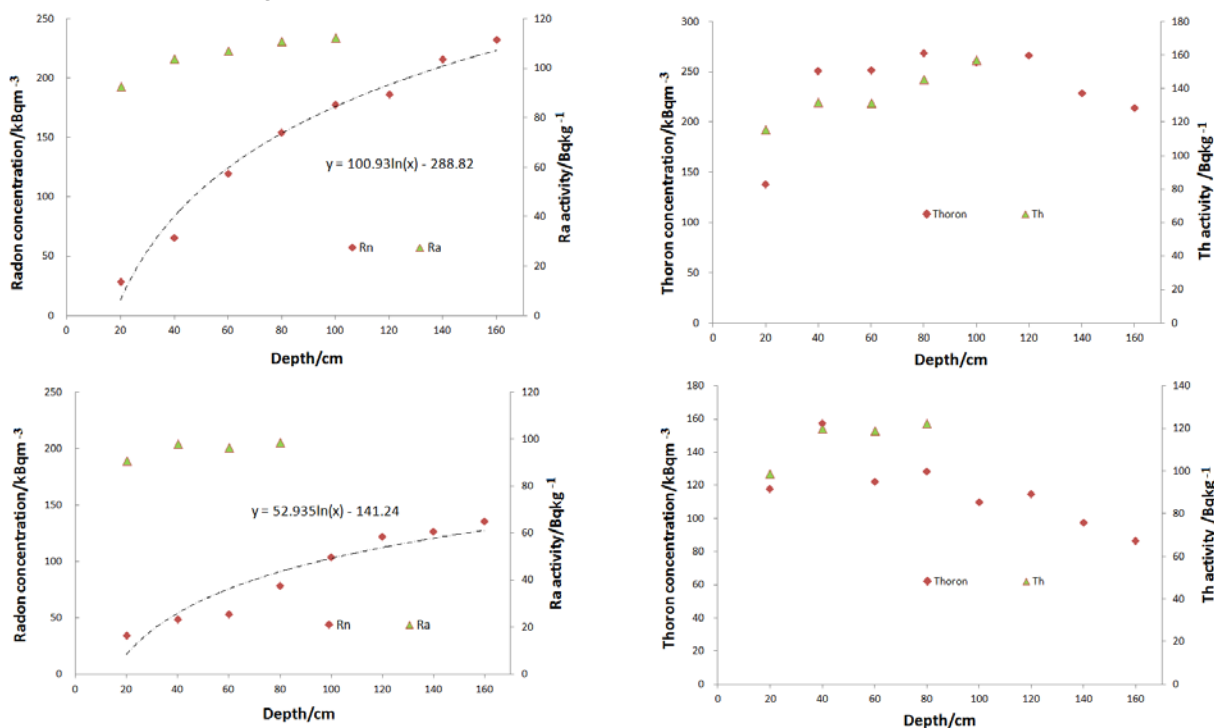


Fig. 2. Radon, radium and thorium concentration in the vertical direction.

Table 1. Statistics of radon and thoron concentrations in soil gas in Shenzhen City [$\text{kBq}\cdot\text{m}^{-3}$]

Isotope	Number of measurements	Soil type	Mean	SD	Min	Max
Radon	35	S	43	22	15	118
	34	WG	130	79	40	370
	69		86	72	15	370
Thoron	35	S	49	23	2.2	96
	34	WG	188	66	103	435
	69		118	85	2.2	435

SD: standard deviation; S: sediments, including sand, mudstone, siltstone, clay, tuff, rhyolite, and schist; WG: weathered granite and monzogranite.

Table 2. Statistical correlation between radon, thoron and lithology

		Radon	Thoron	Lithology
Radon	Pearson correlation	1	0.565*	0.610*
	Sig. (2-tailed)		0.000	0.000
	N	69	69	69
Thoron	Pearson correlation	0.565*	1	0.819*
	Sig. (2-tailed)	0.000		0.000
	N	69	69	69
Lithology	Pearson correlation	0.610*	0.819*	1
	Sig. (2-tailed)	0.000	0.000	
	N	69	69	69

N: number of samples; * Correlation is significant at the 0.01 level.

some difference of ^{222}Rn concentration between the two sites. ^{222}Rn concentrations of site LWS are higher than that of site WTS.

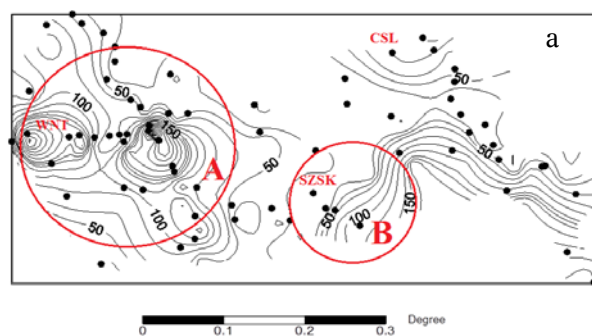
- The distribution of thoron concentration of soil gas in the vertical direction has no obvious regularity, but thoron concentrations of site LWS are higher than that of site WTS.

The relationship between the concentration of radon and thoron in the soil gas and lithology is a problem that we care about because of the extensive exposure of granite rocks in SC. The results of statistical correlation are listed in Table 2. The correlation coefficients in Table 2 display that $^{222}\text{Rn}/^{220}\text{Rn}$ concentration in soil gas is significantly related to lithology.

Distribution of $^{222}\text{Rn}/^{220}\text{Rn}$

The total of 69 measurement locations was designed at the location of the grid nodule, a grid of $10\text{ km} \times 10\text{ km}$, where we carried out the radon survey in SC.

The statistics of $^{222}\text{Rn}/^{220}\text{Rn}$ concentrations of the total of 69 locations are listed in Table 1. The mean values of $^{222}\text{Rn}/^{220}\text{Rn}$ concentration are the same level in the areas of weathered granite and sediments and weathered rhyolite, but $^{222}\text{Rn}/^{220}\text{Rn}$ concentrations vary intensely in the areas of weathered granite. The maximum of $^{222}\text{Rn}/^{220}\text{Rn}$ concentration was $370\text{ kBq}\cdot\text{m}^{-3}$ and $435\text{ kBq}\cdot\text{m}^{-3}$, respectively.



Geographical distribution characteristics

Based on the $^{222}\text{Rn}/^{220}\text{Rn}$ concentration of the measured data in SC, $^{222}\text{Rn}/^{220}\text{Rn}$ contour maps were compiled using Kringing interpolation, shown in Fig. 3. Comprehensive analyses of Fig. 1 and Fig. 3, we can draw the following understanding:

- $^{222}\text{Rn}/^{220}\text{Rn}$ concentrations in soil gas were higher in the west of SC where dominated by monzogranite of the Middle Cretaceous, and in the south of SC extensively developed biotite granite of the Later Jurassic, marked A and B.
- The maximum ^{220}Rn concentration ($450\text{ Bq}/\text{m}^3$)

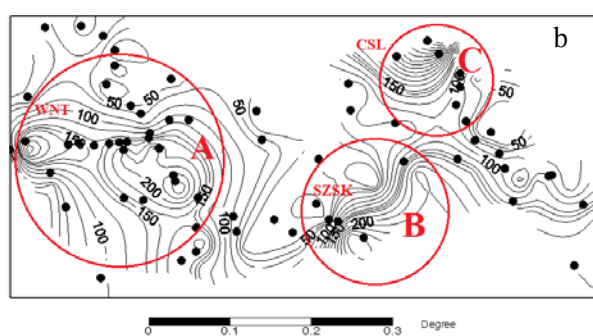


Fig. 3. Contour map of radon and thoron concentration in soil gas in Shenzhen City. (a) Radon contour map. (b) Thoron contour map.

was observed at site CSL located in a litchi orchard in the northeast zone covered with the weathered products of the Later Jurassic biotite granite rocks. The maximum value of ^{222}Rn concentration (370 Bq/m^3) was observed at site SL located in the west part of SC.

- $^{222}\text{Rn}/^{220}\text{Rn}$ concentrations were not high in the areas exposed sandstone, mudstone, siltstone, tuff, and other kind of sediments. These districts include the middle parts of SC.

Conclusions and suggestions

Our preliminary radon investigations show that:

- The characteristics and distributions of $^{222}\text{Rn}/^{220}\text{Rn}$ concentration of soil gas in SC are obviously related to lithology. High $^{222}\text{Rn}/^{220}\text{Rn}$ concentrations were mainly observed in the outcrops of weathered granite.
- The distribution of ^{222}Rn concentration in the vertical direction displays an exponential distribution mode, but there is no rule of ^{220}Rn concentration.
- We suggest that people should perform a more detailed investigation of the thoron level in the room in SC because there are high activity concentrations of thoron and thorium in SC.

Acknowledgments. The research was co-supported by the National Natural Science Foundation of China (nos. 40174096 and 41274133) and Research Fund for the Doctoral Programme of Higher Education of China (no. 20120022110011).

References

- UNSCEAR. (2000). *Sources and effects of ionizing radiation*. New York: UN.
- Guo, Q., Shimo, M., & Ikebe, M. (1992). The study of thoron and radon progeny concentration in dwellings in Japan. *Radiat. Prot. Dosim.*, 45, 357–359.
- Iida, T., Nurishi, R., & Okamoto, K. (1996). Passive integrating ^{222}Rn and ^{220}Rn cup monitor with CR-39 detector. *Environ. Int.*, 22, S641–S647.
- Cheng, B., Guo, Q., & Sun, Q. (2006). Study on indoor ^{222}Rn , ^{220}Rn progeny in air in high background radiation area of Yangjiang, China. *Radiat. Prot.*, 26, 50–55.
- Wang, Z., Lubin, J., & Wang, L. (1996). Radon measurement in under-ground dwelling from two prefectures in China. *Health Phys.*, 70, 192–198.
- Zhang, L., & Shang, B. (2004). Indoor ^{222}Rn and ^{220}Rn concentration survey in Guangzhou. *Chin. J. Radio Health*, 13, 36–37.
- Jens, W., Sebastian, F., & Xie, Q. (2000). Radon and thoron in cave dwelling (Yan'an, China). *Health Phys.*, 78, 438–444.
- Shang, B., & Cui, H. (2003). Radon and thoron concentrations in traditional cave dwellings and soil beds. *Radiat. Prot.*, 23, 184–188.
- Hutter, A. R. (1996). Spatial and temporal variations of soil gas ^{222}Rn and ^{220}Rn at two sites in New Jersey. *Environ. Int.*, 22, S455–S469.
- Malczewski, D., & Zaba, J. (2007). ^{222}Rn and ^{220}Rn concentration in soil gas of Karkonosze-Izera Block (Sudetes, Poland). *J. Environ. Radioact.*, 92, 144–164.
- Moreno, V., Bach, J., & Font, L. I. (2016). Soil radon dynamics in the Amer fault zone: An example of very high seasonal variations. *J. Environ. Radioact.*, 151, 293–303. <http://dx.doi.org/10.1016/j.jenvrad.2015.10.018>.
- Jaishi, H. P., Singh, S., & Tiwari, R. P. (2014). Temporal variation of soil radon and thoron concentrations in Mizoram (India), associated with earthquakes. *Nat. Hazards*, 72(2), 443–454. DOI: 10.1007/s11069-013-1020-4.
- Jaishi, H. P., Singh, S., & Tiwari, R. P. (2013). Radon and thoron anomalies along Mat fault in Mizoram, India. *J. Earth Syst. Sci.*, 122(6), 1507–1513.
- Catalano, R., Imme, G., & Mangano, G. (2015). In situ and laboratory measurements for radon transport process study. *J. Radioanal. Nucl. Chem.*, 306, 673–684. DOI: 10.1007/s10967-015-4336-6.
- Padilla, G. D., Hernández, P. A., Padrón, E., Barrancos, J., Perez, N. M., Melian, G., Nolasco, D., Rodriguez, F., Calvo, D., & Hernandez, I. (2013). Soil gas radon emissions and volcanic activity at El Hierro (Canary Islands): The 2011–2012 submarine eruption. *Geochem. Geophys. Geosyst.*, 14, 432–447. DOI: 10.1029/2012GC004375.
- Bala Sundar, S., Chitra, N., Vijayalakshmi, I., Danalakshmi, B., Chandrasekaran, S., Jose, M. T., & Venkatraman, B. (2015). Soil radioactivity measurements and estimation of radon/thoron exhalation rate in soil samples from Kalpakkam residential complex. *Radiat. Prot. Dosim.*, 164, 569–574. DOI: 10.1093/rpd/ncv313.
- Syarbaini, & Pudjadi, E. (2015). Radon and thoron exhalation rates from surface soil of Bangka-Belitung Islands, Indonesia. *Indones. J. Geosci.*, 2, 35–42.
- Al-Hamidawi, A. A., Jabar, Q. S., & Al-Mashhadani, A. H. (2012). Measurement of radon and thoron concentrations of soil-gas in Al-Kufa city using RAD-7 detector. *Iraqi J. Phys.*, 10, 110–116.
- Wang, N., Peng, A., & Xiao, L. (2012). The level and distribution of ^{220}Rn concentration in soil-gas in Guangdong Province, China. *Radiat. Prot. Dosim.*, 152(1/3), 204–209. DOI: 10.1093/rpd/ncs223.
- Xiong, S., Wang, N., & Fan, Z. (2012). Mapping the terrestrial air-absorbed gamma dose rate based on the data of airborne gamma-ray spectrometry in southern cities of China. *J. Nucl. Sci. Technol.*, 49, 61–70.
- Durridge Company Inc. (2015). *RAD7 Radon detector. User manual*. Retrieved December 16, 2015, from <http://www.durridge.com/documentation/RAD7Manual.pdf>.
- Kang, Z., Wang, Y., Wang, X., Wei, Y., & Deng, L. (2009). *Shenzhen geology*. Beijing: Geological Publishing House (in Chinese).
- Li, T., Wang, N., & Li, S. (2015). Preliminary investigation of radon concentration in surface water and drinking water in Shenzhen City, South China. *Radiat. Prot. Dosim.*, 167(1/3), 59–64. DOI: 10.1093/rpd/ncv207.